CHEMISTRY
A EUROPEAN JOURNAL

DOI: 10.1002/chem.200600372

Identity S_N2 Reactions $X^- + CH_3X \rightarrow XCH_3 + X^-$ (X = F, Cl, Br, and I) in Vacuum and in Aqueous Solution: A Valence Bond Study

Lingchun Song,[a] Wei Wu,*[a] Philippe C. Hiberty,[b] and Sason Shaik*[c]

Abstract: The recently developed (L. Song, W. Wu, Q. Zhang, S. Shaik, *J. Phys. Chem. A* **2004**, *108*, 6017) valence bond method coupled with a polarized continuum model (VBPCM) has been applied to the identity S_N2 reaction of halides in the gas phase and in aqueous solution. The barriers computed at the level of the breathing orbital VB method (P. C. Hiberty, J. P. Flament, E. Noizet, *Chem. Phys. Lett.* **1992**, *189*, 259), BOVB and VBPCM//BOVB, are comparable to CCSD(T) and CCSD(T)//PCM results and to experimentally derived barriers in solution (W. J. Albery, M. M. Kreevoy, *Adv. Phys. Org. Chem.* **1978**, *16*, 85). The reactivity parameters needed to apply the valence bond state correlation diagram (VBSCD) method (S. Shaik, *J. Am. Chem. Soc.* **1984**, *106*, 1227), were also determined by VB calculations. It has been shown that the reactivity parameters along with their semiempirical derivations provide a satisfactory qualitative and quantitative account of the barriers.

Keywords: ab initio calculations · S_N2 reactions · solvent effects · valence bond theory

Introduction

Nucleophilic substitution (S_N2) reactions have been extensively studied both experimentally[1–8] and theoretically[9–19] because of their great importance in organic chemistry and biological systems. One of the interesting issues in the field is the significant difference between the reactions in the gas phase and in solution.[12,18] In the gas phase, the reactions involve double well potentials with ion–molecule complexes residing in the deep minima of the profile, while in a solvent medium the energy profile is flattened to the verge of eliminating the minima. The other important aspect is that the activation barrier of these reactions is strongly affected by solvent polarity.[7,12] Finally, the S_N2 mechanism is extremely important since it constitutes textbook material that is taught at various levels of chemical education.[20] Understanding the reactivity patterns of S_N2 reactions both in the gas phase and in solution has therefore become a goal of considerable practical and conceptual importance.

As one of the modern theories of chemical bonding, valence bond (VB) theory is a relatively simple and straightforward tool for gaining insights into chemical problems.[21–26] Unfortunately, the use of VB theory for the quantitative assessment of mechanisms has been traditionally hampered by the amount of computer time required for the calculations. This is true in particular for the quantitative modeling of reactions in solution. However, in the last three decades VB theory has been enjoying some resurgence thanks to rapid developments in computer science, which has allowed the inclusion of solvent effects in VB calculations.[27–29] This has given us an opportunity to include solvation effects in the VB calculations of barriers and at the same time to project the insight that VB theory brings into reactivity problems. As such, our approach was two-pronged: 1) initially all the barriers were calculated by means of a VB theory that includes solvation terms and 2) subsequently, the VB state correlation diagram (VBSCD)[30] was used to model and reproduce computed barriers with the aim of gradually establishing a general structure–reactivity expression for this important reaction.

[a] Dr. L. Song, Prof. W. Wu
Department of Chemistry, Center for Theoretical Chemistry
and State Key Laboratory for Physical Chemistry of Solid Surfaces
Xiamen University, Xiamen, Fujian 361005 (China)
Fax: (+86) 592-218-6207
E-mail: weiwu@xmu.edu.cn

[b] Prof. P. C. Hiberty
The Laboratoire de Chimie Physique, Groupe de Chimie Théorique
Université de Paris-Sud, 91405 Orsay Cédex (France)

[c] Prof. S. Shaik
Department of Organic Chemistry and the Lise Meitner-Minerva
Center for Computational Quantum Chemistry
The Hebrew University, Jerusalem 91904 (Israel)
Fax: (+972) 2-6584-680
E-mail: sason@yfaat.ch.huji.ac.il

Supporting information for this article is available on the WWW under http://www.chemeurj.org/ or from the author.

The computational approaches for the inclusion of solvation effects can roughly be divided into two categories, one implicit and the other explicit. The polarizable continuum model (PCM)[31,32] belongs to the first category and is one of the most widely used methods in the framework of dielectric continuum models. Recently, we developed the VBPCM method which incorporates the PCM into modern VB calculations.[27] In a similar fashion to the MO-based PCM approaches, the VBPCM method achieves self-consistency between the charge distribution of the solute and the reaction field of the solvent. However, the VBPCM method has an important conceptual bonus since it enables us to compute energy profiles for the full state as well as for the individual VB structures. In so doing, the VB calculations reveal the effect of solvent on the constituents of the wave function, thereby providing a useful insight into the reaction in solution.

Although many S_N2 reactions have been studied extensively by theoretical methods,[12,18] this was not done using VB theory, and especially not by the use of the higher levels of VB methodology. To our knowledge, except for recent MO-VB-type calculations,[29] there has been no pure ab initio VB study of S_N2 reactions that has included solvent effects. The aim of this study was to apply breathing orbital VB (BOVB)[33] and VB configuration-interaction (VBCI)[34] methods coupled with the recently developed VBPCM method[27] to understand the origin of barriers and their dependence on the nature of X in identity S_N2 reactions [Eq. (1)].

$$X^- + CH_3X \rightarrow XCH_3 + X^- \quad (X = F, Cl, Br, I) \tag{1}$$

This paper is organized as follows: It starts with brief reviews of the VB methodologies employed. The VB computational results for the reaction in the gas phase are reported in the next section and these are followed by the results of calculations in solution. Subsequently, the application of the VBSCD model to the origin of the reaction barriers and their dependence on the identity of the halogen is reported.

Theory and Methodology

VB procedures: In VB theory, the state wave function, Ψ, is expressed as a linear combination of VB structures, Φ [Eq. (2)], where Φ_K are VB structures that correspond to all the modes of distributing the "active electrons" that participate in the interchanging bonds and c_K are the corresponding structural coefficients.

$$\Psi = \sum_K c_K \Phi_K \tag{2}$$

In the VBSCF procedure,[35] both the VB orbitals and the structural coefficients are optimized simultaneously to minimize the total energy. As such, the VBSCF method takes care of the static electron correlation; however, it lacks the dynamic correlation that is absolutely essential for obtaining quantitative accuracy.

The breathing orbital VB (BOVB)[33] method improves the VBSCF method by introducing a dynamic correlation. In the BOVB method, the orbitals are allowed to be different for different VB structures. In this manner, the orbitals respond to the instantaneous fields of the individual VB structures rather than to an average field of all the structures. As such, the BOVB method accounts for part of the dynamic correlation, while leaving the wave function as compact as in the VBSCF method.

The VB configuration-interaction (VBCI)[34] method uses a configuration interaction technique to account for the missing dynamic correlation in a VBSCF[35] calculation. A VBCI calculation involves the entire set of fundamental and excited VB structures. In a similar manner to MO-based CI methods, in the VBCI method, the excited VB structures are generated by replacing occupied orbitals with virtual orbitals. The virtual orbitals are strictly localized on precisely the same fragment as the corresponding occupied orbitals. In this manner, by merging all the excited VB structures into the corresponding elementary structure of the same electron occupancy and pairing, the entire VBCI wave function is condensed to a linear combination of the same minimal number of VB structures as in the VBSCF and BOVB methods.

The weights (w) of the VB structures are determined by use of the Coulson–Chirgwin formula[36] [Eq. (3)], which is the equivalent of a Mulliken population analysis in VB theory.

$$w_K = {c_K}^2 + \sum_{L \neq K} c_K c_L \langle \Phi_K | \Phi_L \rangle \tag{3}$$

The VB structure set: For an S_N2 reaction, structures **1**–**6** in Scheme 1 describe all the possible ways of distributing the four electrons of the anion $X:^-$ and the H_3C–X bond among the three fragments (X, CH_3, X). Structures **1** and **4** correspond to the covalent Heitler–London (HL) structures, which describe the spin pairing in the C–X bonds of the reactants and products, respectively. Structure **3** is the most stable triple-ion configuration with a positive charge on the central methyl moiety and one negative charge on each halogen atom. In structure **5**, known as the "long-bond structure", the odd electrons on the two X atoms are spin-paired

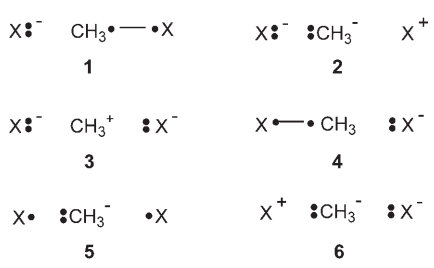

Scheme 1. VB structures for the S_N2 reaction.

and there is a negative charge on the methyl moiety. The remaining structures **2** and **6**, with a negative charge placed on the methyl moiety and a positive charge on one of the X atoms, have an unfavorable charge arrangement and are of high energy. The computational study and the discussion of the results in terms of the VBSCD model have been carried out with these six structures. On occasions [see, for example, the derivation of Eq. (18)], approximate quantities can be obtained by considering **1**, **4**, and **3** as the main structures.

The VBPCM method: In the framework of a standard polarizable continuum method, the solute molecule is studied quantum mechanically and the interaction between solute and solvent is represented by an interaction potential, V_R, which is treated as a perturbation on the Hamiltonian of the solute molecule [Eq. (4) and Eq. (5), where H° is the Hamiltonian of the solute molecule in a vacuum, Ψ° and Ψ are the state wave functions of the solute in the gas phase and in solution, respectively, and E° and E are their respective energies]. The interaction potential can be expressed as Equation (6), where the first term depends explicitly on the wave function of the solute, while the second term is independent of the wave function. Equation (5) can be solved by minimizing the function G by using the constraint condition $\langle\Psi|\Psi\rangle=1$ [Eq. (7)]. The contribution to the interaction potential is usually given by the sum of electrostatic, dispersion, and repulsion components [Eq. (8)]. In principle, the above three terms depend on the charge distribution of the solute. However, for simplicity, the treatment reduces the interaction potential to the electrostatic component in the QM calculation, while the contributions from the other terms are based on empirical parameters. Therefore, the total free energy can be written as in Equation (9), where V_{NN} is the nuclear repulsion energy and G_{nel} stands for the contributions from nonelectrostatic components. The factor of $^1/_2$ that multiplies $\langle V'_R\rangle$ accounts for the energy change in the solvent as a result of its polarization by the solute.

$$H^\circ\Psi^\circ = E^\circ\Psi^\circ \tag{4}$$

$$(H^\circ + V_R)\Psi = E\Psi \tag{5}$$

$$V_R = V'_R(\Psi) + V''_R \tag{6}$$

$$G = \langle\Psi|H^\circ + V''_R + \frac{1}{2}V'_R(\Psi)|\Psi\rangle \tag{7}$$

$$V_R = V_{el} + V_{dis} + V_{rep} \tag{8}$$

$$G = \langle\Psi|H^\circ|\Psi\rangle + \langle\Psi|V''_R|\Psi\rangle + \frac{1}{2}\langle\Psi|V'_R(\Psi)|\Psi\rangle + V_{NN} + G_{nel} \tag{9}$$

To implement the PCM in a VB scheme, the VBPCM method expands the state wave function, Ψ, in terms of the usual VB structures, as in Equation (2). And, now, these VB structures are optimized and allowed to interact with one another in the presence of a polarizing field of the solvent. In a similar fashion to the MO-based PCM method, the interaction between the solute and the solvent depends on the electron density of the solute and is expressed in the form of one-electron integrals which are used in the standard PCM procedure. Adding the integrals to the original electronic integrals, a standard VB procedure then follows and optimizes the VB orbitals. The final energy of the system in solution is given by Equation (10).

$$E = \langle\Psi|H^\circ + \frac{1}{2}V_R|\Psi\rangle \tag{10}$$

By performing the above procedures, the solvent effect is taken into account in the VB calculations. The type of calculation will be henceforth designated by the level of calculation, for example, as VBPCM//VBSCF, VBPCM//BOVB, or VBPCM//VBCI.

Computational Details

In this paper, the PCM part of the calculation was performed with the GAMESS[37] package (version: 20 June 2002 (R2)) and the VB part was carried out using the Xiamen VB (XMVB)[38] package. An interface was written to transfer to input/output files between the two codes.

The integral equation formalism (IEF) PCM model[39] was adopted in this work. In our previous work that introduced the VBPCM method, the molecule cavity was defined in terms of van der Waals radii. However, test calculations showed that the use of van der Waals radii does not provide good quantitative accuracy for the dissociation energy curves of C–X bonds produced by the VBPCM method. By using VB theory with inclusion of solvation effects, the bond dissociation curves result in heterolytic cleavage of the bond to C^+ and X^-. As such, taking constant values for the atomic radii along the reaction coordinate, as was done before, grossly elevates the energy of the ionic fragments and the "more ionic" parts of the curves. A more careful treatment should use variable values, depending on the charges of the fragments, as a function of the progress along the reaction coordinate. In this work, we used the UAHF model of Tomasi and co-workers.[40] In this model the atomic radii of the spheres used to build the molecular cavity are adjusted by introducing chemical considerations such as hybridization, formal charge, and the first-neighbor inductive effect. Thus the correction for the atomic radius is given by Equation (11), where q is the formal charge carried by the atom at a given point of the reaction coordinate and r_q is a scale factor that is different for anions and cations. In this work, the values of q were taken from the Mulliken charge given by CCSD(T) calculations in the gas phase. Hence, different values of atomic radii were used for the reactant and transition state. For example, for the identity S_N2 reaction with X = F, the value of R(F) is 1.50 Å for the neutral fluorine atom in the reactants, $R(F^-)$ is 1.20 Å for the anion, and 1.27 Å in the transition state (TS) for which the fluorine Mulliken charge is −0.53. The atomic radii are listed in Table S1 of the Supporting information.

$$R'(X) = R(X) + r_q|q| \tag{11}$$

To obtain quantitative accuracy, the gas-phase calculations were carried out with the BOVB method, and the solution phase study with VBPCM//BOVB. The inner electrons were frozen at the Hartree–Fock level, leaving 22 valence electrons (10 σ electrons and 12 π electrons) to be treated in the VB computation. Test calculations showed that dynamic correlation of the π electrons varies very little along the entire reaction path. To reduce the computational cost, in the BOVB calculation, only the σ valence orbitals, which are directly involved in the formation and breakage of the C–X bond, were defined as "breathing orbitals". The other orbitals remained common to all the VB structures.

The 6-31G* basis set was employed for the H, C, F, and Cl atoms, while for the Br and I atoms we used the Los Alamos effective core potential and matching basis set, LANL2DZ,[41] to which we added d-polarization functions taken from the literature[42] (henceforth ECP-31G*). The barrier calculations performed with the 6-31+G* basis set were subsequently used to test the basis set dependence of the VB computed barriers.

The geometries of the CH_3–X molecules, the ion–molecule complexes $X^-\cdots CH_3$–X, and the transition states (listed in Table 1) were optimized at the MP2 level of theory. In the gas phase, the ion–molecule complex is considered to be the reactant state and the calculated reaction barrier refers to the "central barrier" between the reactant and product complex. On the other hand, no such complex exists in the aqueous phase, and the reactant state is made up of the separate X^- and CH_3–X species. As the geometric relaxation of the transition states and CH_3–X molecules was found to be rather small in aqueous solution, the gas-phase geometries were kept unchanged for the VBPCM//BOVB calculations.

Table 1. C–X bond lengths [Å] for the CH_3–X molecules, the respective ion–molecule clusters (RS), and the transition states of the identity reactions.[a]

X	CH_3–X	RS (gas phase)	TS $(X\cdots CH_3\cdots X)^-$
F	1.393	1.443, 2.429	1.784
Cl	1.778	1.814, 3.163	2.310
Br	1.945	1.982, 3.270	2.463
I	2.144	2.180, 3.533	2.669

[a] Calculated at the MP2/6-31G* (X=F, I) and MP2/ECP-31G* (for X=Br, I) level of theory.

Results

The reaction barriers in the gas phase are listed in Table 2a,b. It can be seen from Table 2a that the results of the MO-based calculations, HF, MP2, and CCSD(T), are in good agreement with each other. The trend in the values of the barriers is F<Cl>Br>I. The VBSCF barriers are much higher than those of the MO-based methods and the trend in the barriers is different. The barriers of the higher levels of the VB methods, BOVB, VBCIS, and VBCISD, are improved relative to the simple VBSCF method and are in good agreement with one another and with the MO-based results.

Table 2b shows the barriers determined with the 6-31+G* basis set. It can be seen that these barriers are slightly higher than the corresponding values obtained with the 6-31G* basis set, but all the trends remain the same. For the sake of simplicity, we focus henceforth on the BOVB results.

Table 2. S_N2 reaction barriers [kcal mol^{-1}] in the gas phase computed with various methods.

	HF	MP2	CCSD(T)	VBSCF	BOVB	VBCIS	VBCISD
a) 6-31G*							
F	11.6	11.5	11.3	25.4	14.0	12.6	13.4
Cl	14.2	15.3	13.7	21.2	14.0	13.1	13.9
Br	11.3	11.7	10.5	15.9	11.4	11.0	11.5
I	10.5	10.0	9.1	14.3	10.4	10.2	10.7
b) 6-31+G*							
F	17.7	12.2	12.0	30.4	14.1		
Cl	15.8	17.0	15.3	22.7	14.3		
Br	13.4	13.3	11.9	18.4	12.4		
I	12.3	11.4	10.2	16.3	11.3		

Table 3a and b list the reaction barriers in aqueous solution determined by the MO-based and various VBPCM methods with the 6-31G* and 6-31+G* basis sets, respectively. As can be seen from Table 3a, unlike in the gas phase, all the sets of reaction barriers share the same trend, that is, F>Cl>Br>I. Once again, the VBPCM//VBSCF barriers are relatively high compared with experimental values,[7] while the VBPCM//BOVB barriers provide excellent agreement with experiment. Table 3b lists the barriers determined with the 6-31+G* basis set and shows that the values of the barriers for X=F for all methods are higher than the corresponding values obtained with the 6-31G* basis set, while for X=I, the 6-31+G* quantities are a bit lower than those determined with 6-31G*. However, the deviations can still be considered acceptable.

Table 3. S_N2 reaction barriers [kcal mol^{-1}] in aqueous solution.

	HF	MP2	CCSD(T)	VBSCF	BOVB	exptl[a]
a) 6-31G*						
F	37.9	28.6	28.6	52.3	32.0	31.8
Cl	28.6	30.1	28.6	36.1	26.8	26.5
Br	24.3	24.6	23.7	30.3	23.8	23.7
I	22.5	22.4	21.8	32.7	22.6	23.2
b) 6-31+G*						
F	38.9	30.4	30.2	51.3	37.7	
Cl	28.8	29.3	27.6	34.7	26.1	
Br	20.9	21.8	20.6	26.5	21.0	
I	20.0	20.2	19.2	24.5	20.3	

[a] Ref. [7].

Table 4 lists the solvation energies of all the species. The solvation energies of X^- are fairly close to the experimental values.[43,44] Thus, the PCM method affords good quantitative comparison with experiment for ionic solvation. Hence, coupled with BOVB, the VBPCM method yields reasonable barrier data. On the other hand, the nonequilibrium solvation values for the CH_3X^- species are almost comparable to the equilibrium values, while they should be much lower, by almost a factor of 2.[12] Generally speaking, continuum-based solvation models cannot treat nonequilibrium solvation well unless some construction is added to change the dielectric constant of the solvent between the static and optical limits.[12] This will pose some constraints on the application of the VBSCD method with VBPCM values to the solvation of the CH_3X^- species (see later).

Table 5 and Table 6 give the weights of the six VB structures [see Eq. (3)] described in Scheme 1. It can be seen that the weights of the two covalent structures **1** and **4** are significant, but it is the triple-ion structure **3** that makes the most important contribution to the wave function of the TS for all systems. The weight of this structure decreases in the order of descending X electronegativity. The weights of structures **2** and **6** are virtually zero as the charge distribu-

Table 4. Desolvation energies of all species [kcal mol^{-1}].[a]

	Neutral 6-31G*	Anion 6-31G*	Anion 6-31+G*	$-\Delta G_{hyd}^{\circ}$ (X^-)[b]
F	0.3	111.5	102.8	113 (104.3)
Cl	0.5	77.3	73.5	83
Br	0.6	72.7	67.7	77
I	0.6	63.4	60.0	68
CH_3F	2.7	67.0 (64.7)[c]		
CH_3Cl	2.1	64.6 (60.6)[c]		
CH_3Br	2.1	62.7 (59.1)[c]		
CH_3I	1.8	56.9 (53.5)[c]		
TS(F)	–	72.4		
TS(Cl)	–	57.1		
TS(Br)	–	52.7		
TS(I)	–	46.5		

[a] The desolvation energies refer to the process X(aq)→X(g), where X is one of the species in the Table. [b] These absolute $-\Delta G_{hyd}^{\circ}$ values are taken from ref. [43]. The value in parentheses for F^- is from ref. [44]. [c] The values not in parentheses refer to equilibrium solvation values. Those in parentheses are the solvation energies calculated using the same radii as the ground states species, that is, CH_3X^- has the same radius as CH_3X.

Table 5. Weights of VB structures[a] obtained by BOVB calculations in the gas phase.

X	Species[b]	**1**	**2**	**3**	**4**	**5**	**6**
F	TS	0.228	0.002	0.507	0.228	0.033	0.002
	RS	0.492	0.046	0.462	0.000	0.000	0.000
Cl	TS	0.253	0.003	0.451	0.253	0.036	0.003
	RS	0.612	0.121	0.267	0.000	0.000	0.000
Br	TS	0.273	0.003	0.403	0.273	0.045	0.003
	RS	0.634	0.102	0.265	0.000	0.000	0.000
I	TS	0.293	0.004	0.351	0.293	0.055	0.004
	RS	0.653	0.139	0.208	0.000	0.000	0.000

[a] The structure numbers are shown in Scheme 1. The basis set is 6-31G*. [b] TS is the transition state, RS is the reactant state.

Table 6. Weights of VB structures[a] obtained by BOVB calculations in aqueous solution.

X	Species[b]	**1**	**2**	**3**	**4**	**5**	**6**
F	TS	0.216	0.002	0.537	0.216	0.028	0.002
	RS	0.481	0.029	0.490	0.000	0.000	0.000
Cl	TS	0.239	0.003	0.488	0.239	0.029	0.003
	RS	0.640	0.097	0.263	0.000	0.000	0.000
Br	TS	0.261	0.002	0.436	0.261	0.038	0.002
	RS	0.659	0.079	0.262	0.000	0.000	0.000
I	TS	0.285	0.004	0.375	0.285	0.048	0.004
	RS	0.688	0.117	0.195	0.000	0.000	0.000

[a] The structure numbers are shown in Scheme 1. The basis set is 6-31G*. [b] TS is the transition state, RS is the reactant state.

tion pattern of these structures is the most disfavored among the VB structures. The weights of structure **3** for all the X atoms are higher in aqueous solution (Table 6) than in the gas phase. This trend makes physical sense as the solvent affects the energies of the polar structures more than those of the covalent structures.

Because the weights of the two covalent structures are equal in the transition states, and since the reactant state is dominated by a single covalent structure, it is clear that the VB calculations correspond to a VB avoided-crossing situation as described originally by the VBSCD model.[30] The VBSCD model has been amply discussed in the literature and Figure 1 illustrates the corresponding diagrams for the identity reaction in the gas (Figure 1a) and aqueous phases (Figure 1b). In these diagrams, the barrier arises from the

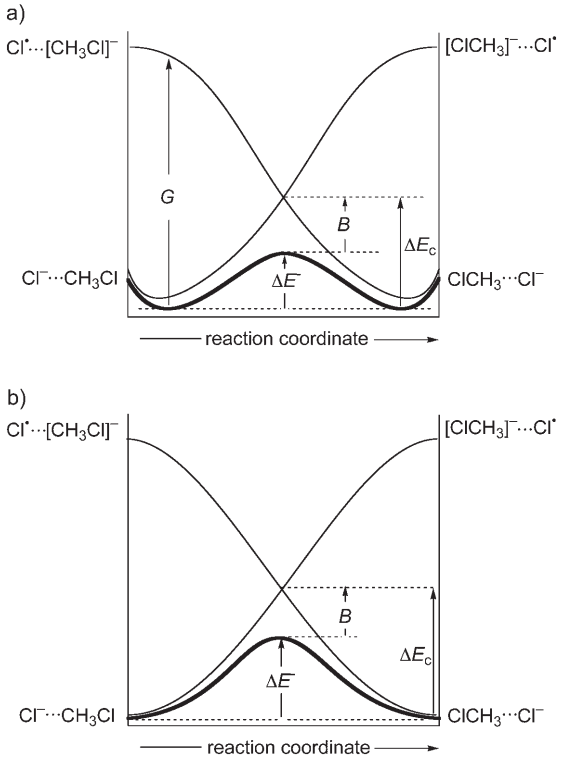

Figure 1. A qualitative curve crossing diagram for the identity S_N2 process: $X_1+CH_3X_r \rightarrow X_1CH_3+X_r$ ($X_1=X_r=$F, Cl, Br, I). a) Gas phase; b) aqueous phase.

avoided crossing of two diabatic curves, one representing the energy variation of the reactant's diabatic state along the reaction coordinate, the other representing the product's state. Thus, the reactant's diabatic curve is calculated as an optimized mixture of structures **1**, **2**, **3**, and **5**, while the product's diabatic curve is made up of structures **3**, **4**, **5**, and **6**. Both diabatic curves rise continuously from their minimum and correlate with the respective charge-transfer state ($X^{\bullet}+CH_3X^-$, where structure **5** mixes in to delocalize the extra electron in the CH_3X^- species). As such, the two curves cross in the middle of the diagram. At the crossing point, the diabatic curves mix to generate the ground state of the transition state, which is the top of the reaction profile (dark curve) in Figure 1a,b. The quantities that determine the barrier height are the promotion gap, *G*, which is the charge-transfer energy, the fraction *f* of the gap that is below the crossing point, and the resonance energy, *B*, of the transition state. Thus, a general expression for the barri-

er is given by Equation (12), which can be used to estimate the values of the central barriers.

$$\Delta E^{+} = fG - B \tag{12}$$

Table 7 lists the computed parameters of the VBSCD in the gas phase. The promotion gap, G, is the difference between the energy of the reactant state (the ion–molecule complex in the gas phase, the separate reactants in the aqueous phase) and the energy of the charge-transfer state. It is seen that, in accord with qualitative considerations, this quantity is around twice the bond energy of CH_3–X.[30] The resonance energy B is 29.2 kcal mol^{-1} for the reaction with X = F, while for X = Cl, Br, and I, it is around 20–21 kcal mol^{-1}. These values are not too far from previous estimates based on semiempirical treatments of the VBSCD.[45]

Table 7. Computed parameters of the VBSCD method in the gas phase (BOVB/6-31G*).[a]

VBSCD quantity	F	Cl	Br	I
B	29.2	21.2	21.1	20.2
G	218.9	194.6	164.6	129.0
ΔE_c	43.2	35.2	32.4	30.6
f	0.197	0.181	0.197	0.237
D(BOVB)	101.1	76.3	63.8	54.7
D[CCSD(T)]	105.2	78.4	68.7	58.4
ΔE_{ST}[b]	241.7	167.4	137.3	108.8
D(TS)[b]	66.7	46.1	41.7	35.6
ΔE_{ST}(TS)[b]	114.2	73.5	63.3	53.4

[a] All energies in kcal mol^{-1}. [b] CCSD(T) values.

The VB-computed parameters in aqueous solution are collected in Table 8. It can be seen that the solvent has the effect of increasing the G values and consequently also the corresponding heights of the crossing points (ΔE_c). The rise in G is due to the impaired solvation of the charge-transfer excited states in Figure 1 relative to the reactant state (compare the solvation energies of the CH_3X^- anions with those of the X^- anions in Table 4), and this carries over to the ΔE_c values, and hence also to the transition states. From Table 8 we also find the resonance energies of the transition states in aqueous solution to be around 3–4 kcal mol^{-1} smaller than those in the gas phase (Table 7). This illustrates that the solvent effect modulates the mixing energy due to the interaction between the two Lewis structures. This reduction in resonance energy follows previous qualitative analyses with the VBSCD,[30b,45,46] which predicted that whenever the transition state acquires a higher triple-ion character its resonance energy will diminish. Nevertheless, modulation of the resonance energy of the TS is small and one is still justified in neglecting this effect in qualitative considerations.

Table 8. Parameters computed with the VBSCD method in aqueous solution (VBPCM//BOVB, 6-31G*).[a]

VBSCD quantity	F	Cl	Br	I
B	25.1	16.9	17.8	16.3
G	268.0	222.6	188.6	145.2
ΔE_c	57.1	43.7	41.6	38.8
f	0.213	0.196	0.221	0.267
D[b]	108.0	83.4	71.5	61.1
ΔE_{ST}[b]	243.7	168.2	137.9	109.3

[a] All energies in kcal mol^{-1}. [b] CCSD(T) values.

Discussion

By using the recently developed semiempirical VB theory,[30a,47] we can derive an expression for B by using the mixing of the two covalent VB structures **1** and **4** [Eq. (13) and Eq. (14)]. Here Φ^{r}_{HL} and Φ^{p}_{HL} are the covalent structures of the reactants and products, respectively, the orbitals a, b, and c are the active orbitals of the nucleophile, central carbon, and leaving group, respectively, and N_{HL} is a normalization factor. If one neglects the long-range overlap s_{ac} and monoelectronic Hamiltonian matrix element h_{ac}, as well as the higher order products (e.g., overlap squared, like $s_{ab}{}^2$, $s_{ab}s_{bc}$), one has Equation (15), Equation (16), and Equation (17).

$$\Phi^{r}_{HL} = N_{HL}(|a\bar{a}b\bar{c}| - |a\bar{a}\bar{b}c|) \tag{13}$$

$$\Phi^{p}_{HL} = N_{HL}(|c\bar{c}a\bar{b}| - |c\bar{c}\bar{a}b|) \tag{14}$$

$$N_{HL} = \frac{1}{\sqrt{2}} \tag{15}$$

$$S^{rp}_{HL} = \langle \Phi^{r}_{HL} | \Phi^{p}_{HL} \rangle = 4N^{2}_{HL} s_{ab} s_{bc} = 0 \tag{16}$$

$$H^{rp}_{HL} = \langle \Phi^{r}_{HL} | H | \Phi^{p}_{HL} \rangle = 4N^{2}_{HL}(h_{ab}s_{bc} + h_{bc}s_{ab}) = 4h_{ab}s_{bc} \tag{17}$$

The difference between the positive and negative combinations of the two functions is given by Equation (18).

$$\Delta E = \frac{2(H^{rp}_{HL} - E^{r}_{HL}S^{rp}_{HL})}{1-(S^{rp}_{HL})^2} = -2H^{rp}_{HL} = -8h_{ab}s_{bc} \tag{18}$$

While a precise treatment requires the inclusion of all six VB structures, one can still obtain a reasonable approximation for B by also including the triple-ionic structure **3**, Φ_I, which is the most important VB structure. Based on the results of the structural weights (Table 6) we can suppose that the wave function of the TS is expressed by a combination of only three structures, **1**, **3**, and **4**, given by Equation (19), with Φ_1 and Φ_2 expressed by Equation (20). The normalization factors N_1 (N_2) are given by Equation (21).

$$\Psi = N[\Phi_1 + \Phi_2] = N[\Phi^{r}_{HL} + \Phi^{p}_{HL} + \lambda\Phi_I] \tag{19}$$

$$\Phi_1 = N_1[\Phi^{r}_{HL} + \frac{\lambda}{2}\Phi_I] \tag{20a}$$

$$\Phi_2 = N_2[\Phi^{p}_{HL} + \frac{\lambda}{2}\Phi_I] \tag{20b}$$

$$N_1 = N_2 = \frac{2}{\sqrt{4+4\lambda S+\lambda^2}}, \qquad S = \langle \Phi^{r}_{HL}|\Phi_I\rangle \approx 0.40 \tag{21}$$

Recalling the fact that the overlap between the covalent structures, S^{rp}_{HL}, can be neglected [Eq. (16)], the overlap between the two intersecting states is then given by Equation (22).

$$S_{12} = \langle \Phi_1|\Phi_2\rangle = \frac{4\lambda S+\lambda^2}{4+4\lambda S+\lambda^2} \tag{22}$$

Based on previous considerations,[45,46] the quantity B would be related to the singlet-to-triplet excitation (ΔE_{ST}) of the CH_3–X bond in the transition state's geometry by Equation (23), and thus Equation (24).

$$B = \frac{1}{2}(1-S_{12})\Delta E_{ST} \tag{23}$$

$$B = \frac{2\Delta E_{ST}}{4+4\lambda S+\lambda^2} \tag{24}$$

The parameter λ in Equation (24) can be estimated from the charge on CH_3 through Equation (20) by using Equation (25), where Q is the charge on CH_3 in the TS.

$$\lambda^2 = \frac{2Q}{1-Q} \tag{25}$$

For the sake of simplicity, Equation (24) can be turned to a more compact approximate expression based on the recognition that B decreases with increasing Q, the positive charge on the CH_3 group. One can then show (see the Supporting information for a complete derivation) that B is roughly proportional to $1-Q$, and since the singlet-to-triplet excitation is proportional to the bond dissociation energy,[45–47] one obtains the simple expression given in Equation (26), where D is the corresponding C–X bond energy for the CH_3–X molecule in the reactant state and a factor of 0.5 is chosen so as to best fit the accurately calculated values of B.

$$B = (1-Q)0.5D \tag{26}$$

According to the results of ab initio VB calculations, the overlap integral S [between the covalent (HL) and ionic structures; see Eq. (21)] is around 0.4 for the entire series, and Q can be obtained either from CCSD(T) or BOVB calculations. Then one can estimate the transition-state resonance energy using Equations (24)–(26). Table 9 shows these B values and the ab initio BOVB barriers for comparison. The fit is seen to be reasonably good; thus either Equation (24) or the simpler Equation (26) provides good approximations for estimating the value of the avoided crossing interaction (Figure 1), which is the resonance energy at the transition state.

As has been shown previously,[11a,12,48] the reaction barriers in solution can be estimated from the VBSCD in Figure 1b by considering the effect of the solvent on the promotion energy gap, G. Thus, in the ground state of Figure 1b, one considers a strongly solvated X^- anion and a weakly solvated CH_3X molecule. In the charge-transfer excited state above it, there are two species, $X^{\bullet}$ and CH_3X^-; both are solvated with the same solvent configurations as for the ground state, that is, they are in a state of nonequilibrium solvation. This leads to an increase in the promotion gap relative to that in the gas phase equivalent to the difference between the desolvation energies [S in Eq. (27)] of the ground and excited charge-transfer species. The order of magnitude of the solvent effect on the promotion energy, G, can be estimated by Equation (27).

$$G_s = G_g + S(X^{\bullet -}/CH_3X) - S[X^{\bullet *}/(CH_3X)^{-*}] \tag{27}$$

The asterisk on the excited-state species signifies that the charge-transfer state is in a nonequilibrium solvation. Although this equation does not take into account the fact that the reactant is the ion–molecule complex in the gas phase and separate species in the aqueous phase, one can see that it reproduces fairly well the increase in G due to the solvent effect by comparing the data in Table 7 and Table 8. Now, from the desolvation energies that are collected in Table 4, one can see that the VBPCM accounts only slightly for the nonequilibrium solvation effects by using the same values of the radii [Eq. (11)] for the excited state species as for the corresponding ground state. This is because the method does not account for the large destabilization of the $X^{\bullet *}$ species which possesses the same solvent configuration as the strongly solvated $X^{\bullet -}$ anion in the ground state.[11a,48,49] As such, the promotion gap in a solvent is underestimated by the VBPCM method, and will be so by any method coupled with a continuum solvation model.

We may circumvent this problem and use reliable equilibrium solvation energies to estimate the nonequilibrium values as was done before.[12,48,49] By using Equation (12), the general expression for the reaction barrier, we obtain Equation (28) for the barrier in a solvent.

$$\Delta E^{\neq}_s = fG_s - B \tag{28}$$

Table 9. Resonance energy values, B, calculated from semiempirical Equations (24) and (26).[a]

	$Q_{CCSD(T)}$	Q_{BOVB}	$B_{CCSD(T)}$[b] [Eq. (24)]	B_{BOVB}[b] [Eq. (24)]	$B_{CCSD(T)}$[b] [Eq. (26)]	B_{BOVB}[b] [Eq. (26)]	VB-computed B(BOVB)[c]
F	0.53	0.44	26.4	30.1	24.7	28.3	29.2
Cl	0.45	0.40	19.1	20.5	21.6	22.9	21.2
Br	0.41	0.35	17.4	18.8	20.3	20.7	21.1
I	0.37	0.29	15.5	17.1	18.4	19.4	20.2

[a] For the gas-phase transition states. [b] The subscript signifies the origins of the calculated charge used in the corresponding equation. [c] These are the actual BOVB calculated values.

As has been shown previously[12,48,49] the simplest approximation for the promotion gap in a solvent is given by Equation (29), where S_{X^-} is the desolvation energy of X^- (see Table 4). ρ is the solvent reorganization factor, which can be quantified from the static and optical dielectric constants of the solvent by Equation (30), where $\varepsilon_{opt}=n^2$ and n is the refractive index of the solvent.

$$G_s \approx G_g + 2\rho S_{X^-} \quad (29)$$

$$\rho = (\varepsilon-\varepsilon_{opt})/[\varepsilon_{opt}(\varepsilon-1)] \quad (30)$$

With water as solvent the value of ρ is 0.56. The reorganization factor takes into consideration the fact that the species in the excited state are not solvated in their equilibrium solvent configurations, but in the same ones as the ground-state species beneath them.

By using the barrier expressions Equations (12) and (28) and by assuming the same values of f and B as in the gas phase, we obtain Equation (31) for the barrier in solution, with the first term representing the gas-phase barrier. Table 10 shows barriers calculated by using Equation (31).

Table 10. Barriers estimated in solution using Equation (31), and BOVB calculated and experimental values [kcal mol^{-1}].

	F	Cl	Br	I
$\Delta E^{\neq}_g$[a]	14.0	14.0	11.4	10.4
$\Delta E^{\neq}_s$ [Eq. (31)]	38.6 (36.8[d])	29.7 (29.2[d])	26.6 (26.6[d])	27.2 (27.2[d])
$\Delta E^{\neq}_s$[a]	32.0	26.8	23.8	23.2
$\Delta E^{\neq}_s$[b]	37.7	26.1	21.8	20.3
$\Delta E^{\neq}_s$[c]	31.8	26.5	23.7	23.2

[a] BOVB/6-31G* values. [b] BOVB/6-31+G* values. [c] Experimental values. [d] Barriers not in parentheses/in parentheses use 6-31G*/6-31+G* solvation energy values, S_{X^-}, respectively, in Equation (31).

These estimated values are seen to be in fair agreement with the BOVB barriers, and to be consistently higher by 3–4 kcal mol^{-1}. Some improvement in the semiempirical values can be achieved by considering the reorganization energy term for the geometry of the ion–molecule cluster, and since this term is sensitive to the distance between the centers in between which the charge is transferred, it will be reduced, thereby also reducing the barrier.[11a,49] This however is not absolutely necessary since Equation (31) provides correct trends and reasonable estimates.

$$\Delta E^{\neq}_s = \Delta E^{\neq}_g + 2f\rho S_{X^-} \quad (31)$$

Conclusion

We have investigated the identity S_N2 reaction $X^- + CH_3X \rightarrow XCH_3 + X^-$ (X=F, Cl, Br, and I) in a vacuum and in solution. To our knowledge, this is the first ab initio VB study of S_N2 reactions with inclusion of solvent effects. The BOVB and BOVB//VBPCM methods give reasonable reaction barriers and other VB parameters in both phases. This has enabled VB state correlation diagrams (VBSCD) to be generated quantitatively, which in turn provide an insight into the reaction barriers and solvent effects.

The difference between the reactions in the gas phase and in aqueous solution revealed by these methods shows the correct trends, which make physical sense. In aqueous solution the weighting of the triple-ion structure increases and causes a decrease in the resonance energy. This shows that the solvent effect contributes not only to the energies of the Lewis structures but also to the interaction between the two Lewis structures.

The VBSCD analysis has some affinity with the activation strain model which combines molecular orbital theory and a fragment interaction approach to analyze the barriers of S_N2 and elimination reactions.[50] In this model, solvation effects can be viewed as an interaction between the LUMO of the substrate and the HOMO of the nucleophile. As the latter is stabilized by the solvent, the substrate–nucleophile interaction is weakened, resulting in a higher barrier. This model also predicts that the HOMO–LUMO gap in the transition state is higher in the condensed phase than it is in the gas phase. As the resonance energy of the transition state [the B quantity in Eq. (12)] has been shown to be proportional to the HOMO–LUMO gap,[30b] the activation strain model indirectly confirms our finding that solvation reduces the resonance energy.

Based on the semiempirical VB theory, we have proposed an expression for the resonance energy [Eq. (26)], which has been shown to be a good approximation. A complete semiempirical scheme derived from the VBSCD model, which only requires the properties of the reactants, has also been tested. It produces the reaction barriers quite well (Table 10). Thus, it has been shown that a complex computational scheme can be combined with a qualitative model to reveal the trends of the reaction barriers and show their dependence on the fundamental properties of the reactants.

Acknowledgements

The research carried out at the Xiamen University was supported by the Natural Science Foundation of China. The research carried out at The Hebrew University was supported in part by an Israel Science Foundation (ISF) grant to S.S.

[1] W. N. Olmstead, J. I. Brauman, *J. Am. Chem. Soc.* **1977**, *99*, 4219.
[2] T. Barfknecht, J. A. Dodd, K. E. Salomon, W. E. Tumas, J. I. Brauman, *Pure Appl. Chem.* **1984**, *56*, 1809.
[3] S. E. Barlow, J. M. van Doren, V. M. Bierbaum, *J. Am. Chem. Soc.* **1988**, *110*, 7240.
[4] S. Gronert, C. H. DePuy, V. M. Bierbaum, *J. Am. Chem. Soc.* **1991**, *113*, 4009.
[5] J.-L. Le Garrec, B. R. Rowe, J. L. Queffelec, J. B. A. Mitchell, D. C. Clary, *J. Chem. Phys.* **1997**, *107*, 1021.
[6] J. K. Laerdahl, E. Uggerud, *Int. J. Mass Spectrom.* **2002**, *214*, 277.
[7] W. J. Albery, M. M. Kreevoy, *Adv. Phys. Org. Chem.* **1978**, *16*, 85.
[8] S. Kato, G. E. Davico, H. S. Lee, C. H. DePuy, V. M. Bierbaum, *Int. J. Mass Spectrom.* **2001**, *210*/211, 223.
[9] A. Dedieu, A. Veillard, *J. Am. Chem. Soc.* **1972**, *94*, 6730.

[10] a) A. A. Viggiano, J. S. Paschkewitz, R. A. Morris, J. F. Paulson, A. Gonzales-Lafont, D. G. Truhlar, *J. Am. Chem. Soc.* **1991**, *113*, 9404; b) W.-P. Hu, D. G. Truhlar, *J. Am. Chem. Soc.* **1994**, *116*, 7797; c) W.-P. Ho, D. G. Truhlar, *J. Am. Chem. Soc.* **1995**, *117*, 10726.
[11] a) S. Shaik, *J. Am. Chem. Soc.* **1984**, *106*, 1227; b) S. Shaik, A. Ioffe, A. C. Reddy, A. Pross, *J. Am. Chem. Soc.* **1994**, *116*, 262.
[12] S. Shaik, H. B. Schlegel, S. Wolfe, *Theoretical Aspects of Physical Organic Chemistry: The S_N2 Mechanism*, Wiley, New York, **1992**.
[13] a) M. N. Glukhovtsev, A. Pross, L. Radom, *J. Am. Chem. Soc.* **1995**, *117*, 2024; b) M. N. Glukhovtsev, A. Pross, H. B. Schlegel, R. D. Bach, L. Radom, *J. Am. Chem. Soc.* **1996**, *118*, 11258.
[14] J. J. Blavins, D. L. Cooper, P. B. Karadakov, *J. Phys. Chem. A* **2004**, *108*, 914.
[15] L. Deng, V. Branchadell, T. Ziegler, *J. Am. Chem. Soc.* **1994**, *116*, 10645.
[16] S. Schmatz, P. Botschwina, H. Stoll, *Int. J. Mass Spectrom.* **2000**, *201*, 277.
[17] a) H. Wang, W. Hase, *J. Am. Chem. Soc.* **1995**, *117*, 9347; b) Y. Wang, W. L. Hase, H. J. Wang, *J. Chem. Phys.* **2003**, *118*, 2688.
[18] a) G. Vayner, K. N. Houk, W. L. Jorgensen, J. I. Brauman, *J. Am. Chem. Soc.* **2004**, *126*, 9054; b) J. Chandrasekar, S. F. Smith, W. L. Jorgensen, *J. Am. Chem. Soc.* **1984**, *106*, 3049; c) J. Chandrasekar, S. F. Smith, W. L. Jorgensen, *J. Am. Chem. Soc.* **1985**, *107*, 154; d) J. Chandrasekar, W. L. Jorgensen, *J. Am. Chem. Soc.* **1985**, *107*, 2974.
[19] Y. Chen, L. Song, W. Wu, Q. Zhang, *Chem. J. Chin. Univ.* **2003**, *24*, 2227.
[20] See, for example: T. H. Lowry, K. S. Richardson, *Mechanism and Theory in Organic Chemistry*, 3rd ed., Harper and Row, New York, **1987**.
[21] W. A. Goddard, L. B. Harding, *Annu. Rev. Phys. Chem.* **1978**, *29*, 363.
[22] J. H. van Lenthe, G. G. Balint-Kurti, *J. Chem. Phys.* **1983**, *78*, 5699.
[23] D. L. Cooper, J. Gerratt, M. Raimondi, *Adv. Chem. Phys.* **1987**, *69*, 319.
[24] R. McWeeny, *Int. J. Quantum Chem.* **1988**, *34*, 25.
[25] P. Maître, P. C. Hiberty, G. Ohanessian, S. S. Shaik, *J. Phys. Chem.* **1990**, *94*, 4089.
[26] *Valence Bond Theory* (Ed.: D. L. Cooper), Elsevier Science, Amsterdam, **2001**.
[27] L. Song, W. Wu, Q. Zhang, S. Shaik, *J. Phys. Chem. A* **2004**, *108*, 6017.
[28] A. Shurki, H. A. Crown, *J. Phys. Chem. B* **2005**, *109*, 23638.
[29] a) Y. Mo, J. Gao, *J. Comput. Chem.* **2000**, *21*, 1458; b) Y. Mo, J. Gao, *J. Phys. Chem.* **2000**, *104*, 3012.
[30] a) S. Shaik, P. C. Hiberty, *Adv. Quantum Chem.* **1995**, *26*, 99; b) S. Shaik, A. Shurki, *Angew. Chem.* **1999**, *111*, 616; *Angew. Chem. Int. Ed.* **1999**, *38*, 586.
[31] a) S. Miertus, E. Scrocco, J. Tomasi, *Chem. Phys.* **1981**, *55*, 117; b) S. Miertus, J. Tomasi, *Chem. Phys.* **1982**, *65*, 239; c) M. Cossi, V. Barone, R. Cammi, J. Tomasi, *Chem. Phys. Lett.* **1996**, *255*, 327.
[32] a) M. Cossi, V. Barone, M. A. Robb, *J. Chem. Phys.* **1999**, *111*, 5295; b) M. Cossi, V. Barone, *J. Chem. Phys.* **2000**, *112*, 2427.
[33] a) P. C. Hiberty, J. P. Flament, E. Noizet, *Chem. Phys. Lett.* **1992**, *189*, 259; b) P. C. Hiberty, S. Humbel, C. P. Byrman, J. H. van Lenthe, *J. Chem. Phys.* **1994**, *101*, 5969; c) P. C. Hiberty, S. Shaik, *Theor. Chem. Acc.* **2002**, *108*, 255.
[34] a) W. Wu, L. Song, Z. Cao, Q. Zhang, S. Shaik, *J. Phys. Chem. A* **2002**, *106*, 2721; b) L. Song, W. Wu, Q. Zhang, S. Shaik, *J. Comput. Chem.* **2004**, *25*, 472; c) L. Song, W. Wu, Z. Cao, Q. Zhang, *Chem. J. Chin. Univ.* **2001**, *22*, 1896.
[35] a) J. Verbeek, J. H. van Lenthe, *J. Mol. Struct. (THEOCHEM)* **1991**, *229*, 115; b) J. H. van Lenthe, *Int. J. Quantum Chem.* **1991**, *40*, 201; c) G. G. Balint-Kurti, P. R. Benneyworth, M. J. Davis, I. H. Williams, *J. Phys. Chem.* **1992**, *96*, 4346.
[36] H. B. Chirgwin, C. A. Coulson, *Proc. R. Soc. London Ser. A* **1950**, *2*, 196.
[37] GAMESS software package: M. W. Schmidt, K. K. Baldridge, J. A. Boatz, S. T. Elbert, M. S. Gordon, J. J. Jensen, S. Koseki, N. Matsunaga, K. A. Nguyen, S. Su, T. L. Windus, M. Dupuis, J. A. Montgomery, *J. Comput. Chem.* **1993**, *14*, 1347.
[38] a) XMVB: An Ab Initio Nonorthogonal Valence Bond Program, L. Song, W. Wu, Y. Mo, Q. Zhang, Xiamen University, Xiamen, **1999**; b) L. Song, Y. Mo, Q. Zhang, W. Wu, *J. Comput. Chem.* **2005**, *26*, 514.
[39] a) M. T. Cances, V. Mennucci, J. Tomasi, *J. Chem. Phys.* **1997**, *107*, 3032; b) M. Cossi, V. Barone, B. Mennucci, J. Tomasi, *Chem. Phys. Lett.* **1998**, *286*, 253.
[40] a) M. Cossi, V. Barone, R. Cammi, J. Tomasi, *Chem. Phys. Lett.* **1996**, *255*, 327; b) V. Barone, M. Cossi, J. Tomasi, *J. Chem. Phys.* **1997**, *107*, 3210.
[41] P. J. Hay, W. R. Wadt, *J. Chem. Phys.* **1985**, *82*, 270, 284, 299.
[42] C. E. Check, T. O. Faust, J. M. Bailey, B. J. Wright, T. M. Gilbert, L. S. Sunderlin, *J. Phys. Chem. A* **2001**, *105*, 8111.
[43] Y. Marcus, *Ionic Solvation*, Wiley, New York, **1985**, Table 5.10.
[44] C. G. Zhan, D. A. Dixon, *J. Phys. Chem. A* **2004**, *108*, 2020.
[45] S. Shaik, A. C. Reddy, *J. Chem. Soc., Faraday Trans.* **1994**, *90*, 1631.
[46] S. Shaik, E. Duzy, A. Bartuv, *J. Phys. Chem.* **1990**, *94*, 6574.
[47] a) "A Qualitative Valence Bond Model for Organic Reactions": S. Shaik in *New Theoretical Concepts for Understanding Organic Reactions* (Eds.: J. Bertran, I. G. Csizmadia), NATO ASI Series C, Vol. 267, Kluwer Academic, Dordrecht, **1989**, pp. 165–217; b) W. Wu, D. Danovich, A. Shurki, S. Shaik, *J. Phys. Chem. A* **2000**, *104*, 8744; c) S. Shaik, P. C. Hiberty, *Rev Comput. Chem.* **2004**, *20*, 1.
[48] P. Delahay, *Acc. Chem. Res.* **1982**, *15*, 40.
[49] S. S. Shaik, *Prog. Phys. Org. Chem.* **1985**, *15*, 195.
[50] a) F. M. Bickelhaupt, E. J. Baerends, N. M. M. Nibbering, *Chem. Eur. J.* **1996**, *2*, 196; b) F. M. Bickelhaupt, *J. Comput. Chem.* **1999**, *20*, 114.

Received: April 28, 2006
Published online: July 28, 2006

